# Apaf1-dependent programmed cell death is required for inner ear morphogenesis and growth

**Francesco Cecconi[1], Kevin A. Roth[2], Oleg Dolgov[3], Eliana Munarriz[1], Konstantin Anokhin[3], Peter Gruss[4] and Marjo Salminen[5,*]**

[1]Dulbecco Telethon Institute, Department of Biology, University of Rome 'Tor Vergata', via della Ricerca Scientifica, 00133 Rome, Italy
[2]Department of Pathology, University of Alabama at Birmingham, SC 961E, 1530 Third Avenue South, Birmingham, AL 35294, USA
[3]P. K. Anokhin Institute of Normal Physiology RAMS, 6, Bol. Nikitskaya st, 103009 Moscow, Russia
[4]Department of Molecular Cell Biology, Max-Planck Institute of Biophysical Chemistry, Am Fassberg 11, 37077 Goettingen, Germany
[5]Institute of Biotechnology, University of Helsinki, Viikinkaari 9, 00710 Helsinki, Finland
*Author for correspondence (e-mail: marjo.salminen@helsinki.fi)

*Accepted 19 January 2004*

Development 131, 2125-2135
Published by The Company of Biologists 2004
doi:10.1242/dev.01082

## Summary

**During inner ear development programmed cell death occurs in specific areas of the otic epithelium but the significance of it and the molecules involved have remained unclear. We undertook an analysis of mouse mutants in which genes encoding apoptosis-associated molecules have been inactivated. Disruption of the *Apaf1* gene led to a dramatic decrease in apoptosis in the inner ear epithelium, severe morphogenetic defects and a significant size reduction of the membranous labyrinth, demonstrating that an Apaf1-dependent apoptotic pathway is necessary for normal inner ear development. This pathway most probably operates through the apoptosome complex because caspase 9 mutant mice suffered similar defects. Inactivation of the Bcl2-like (*Bcl2l*) gene led to an overall increase in the number of cells undergoing apoptosis but did not cause any major morphogenetic defects. In contrast, decreased apoptosis was observed in specific locations that suffered from developmental deficits, indicating that proapoptotic isoform(s) produced from *Bcl2l* might have roles in inner ear development. In *Apaf1*$^{-/-}$/*Bcl2l*$^{-/-}$ double mutant embryos, no cell death could be detected in the otic epithelium, demonstrating that the cell death regulated by the anti-apoptotic *Bcl2l* isoform, Bcl-$X_L$ in the otic epithelium is Apaf1-dependent. Furthermore, the otic vesicle failed to close completely in all double mutant embryos analyzed. These results indicate important roles for both Apaf1 and *Bcl2l* in inner ear development.**

Key words: Apoptosis, Bcl2l, Bcl-$X_L$, Bcl-$X_S$, Caspase 9, Proliferation, Otic vesicle closure, Semicircular ducts, Cochlea, Mouse

## Introduction

The normal patterning and morphological development requires precise coordination of cell proliferation, differentiation, and programmed cell death. Several apoptotic pathways are active during development, the mitochondrial pathway being the best defined. This pathway is initiated when, upon receipt of a death signal, cytochrome c is released through the outer mitochondrial membrane to the cytoplasm where it interacts with the apoptotic protease activating factor 1 (Apaf1). Apaf1 activates caspase 9 in the context of a multiprotein complex termed the apoptosome. The apoptosome in turn activates downstream caspases, mainly caspase 3, involved in the proteolytic destruction of the cell (reviewed by Sanders and Wride, 1995; Cecconi and Gruss, 2001). Members of the Bcl2 family are known to either promote or inhibit apoptosis in response to a variety of cell death signals. The anti-apoptotic isoform produced from the Bcl2-like (*Bcl2l*) gene (formerly previously known as *BclX*), Bcl-$X_L$ and Bcl2 can inhibit apoptosis, at least in part, by blocking cytochrome c release, thus preventing apoptosome formation (Kluck et al., 1997; Yang et al., 1997). Bcl2 can also regulate the activation of caspase 2 independently of the apoptosome (Marsden et al., 2002). Pro-apoptotic factors such as Bax, Bad and Bak are known to block the anti-apoptotic effects of Bcl-$X_L$ and Bcl2 through heterodimerization (reviewed by Yuan and Yankner, 2000). To add to the complexity, *Bcl2l* may be alternatively spliced to produce a pro-apoptotic isoform, Bcl-$X_S$, and several anti-apoptotic Bcl2 family members are known to be modulated by protease cleavage that produces C-terminal peptides with pro-apoptotic activity (Basañez et al., 2001; Clem et al., 1998; Fujita et al., 1998). Although the major players in the cytochrome c-dependent apoptotic cascade have been identified, the individual contribution of each component to the development of different organs is largely unknown.

The mammalian inner ear includes specialized vestibular sensory organs for balance and a coiled cochlea for hearing. The early development of the inner ear involves invagination

of the ectodermal placode and its closure to form the otic vesicle. Soon after closure, the otic epithelium undergoes a sequence of complex morphogenetic events to form the membranous labyrinth. The endolymphatic duct extends dorsally and the cochlear duct grows ventrally. The utricle and saccule are separated from each other and from the cochlear duct through deepening constrictions in the ventral vestibular part, whereas the dorsal portion develops into three semicircular ducts through a multi-step process. These ducts first emerge as bilayered epithelial outpocketings. The two opposing layers then approach each other and form a so-called fusion plate, in which the cells first detach from the underlying basement membrane, intercalate and then disappear, creating a hollow duct which further grows out to obtain its adult form and size (Sher, 1971; Martin and Swanson, 1993). The periotic mesenchyme develops in close contact with the otic epithelium and forms the bony otic capsule to surround the membranous labyrinth (Sher, 1971; Martin and Swanson, 1993).

Apoptotic cells have been detected in restricted areas of the developing vertebrate inner ear. These areas include the epithelial cells that transiently connect the surface ectoderm and the otic vesicle during and after its closure, the base of the outgrowing endolymphatic duct, a ventral area above the primordium of the vestibulocochlear ganglion and the ventro-medial wall of the growing cochlear duct (Marovitz et al., 1976; Marovitz et al., 1977; Represa et al., 1990; Fekete et al., 1997; Nikolic et al., 2000). In chicken embryos, apoptosis has also been detected in the fusion plates of the semicircular ducts (Fekete et al., 1997). Apoptosis at the fusion plates has not been detected in mouse or human embryos (Martin and Swanson, 1993; Nishikori et al., 1999).

Although the anatomic distribution of apoptotic cells in the inner ear has been described, the molecular pathways regulating programmed cell death in this structure have not been studied in detail. The *Apaf1* mutant mice die usually perinatally (Cecconi et al., 1998; Yoshida et al., 1998). A few postnatal survivors show a hyperactive behavior that was suspected to be a consequence of inner ear defects, because the brain of these mice appeared completely normal (Honarpour et al., 2000). Postnatal defects have been reported in the inner ear of caspase 3 mutant mice (Takahashi et al., 2001). Here we undertook an analysis of *Apaf1*, *Bcl2l* and caspase 9 mutant mice in order to gain insight into the molecular mechanisms controlling cell death during inner ear morphogenesis. We observed that the majority of the cell death in the inner ear was Apaf1-dependent and most probably occurred through the Apaf1/caspase 9 apoptosome pathway. The lack of apoptosis in *Apaf1* mutant mouse embryos led to widespread defects in epithelial morphogenesis and outgrowth. In contrast, increased apoptosis in *Bcl2l* mutant embryos had no major impact on morphogenesis. However, developmental defects with the latter mutants co-localized with a decrease of apoptosis.

## Materials and methods

### Mouse stocks and strains

The generation and genotyping of *Apaf1*$^{-/-}$, *Bcl2l*$^{-/-}$ and caspase 9$^{-/-}$ mice has been described previously (Motoyama et al., 1995; Kuida et al., 1998; Cecconi et al., 1998; Salminen et al., 1998). The *Apaf1* locus contains a promoterless IRES-*lacZ* cassette and thus the expression of the *lacZ* gene is under the control of *Apaf1* transcription regulatory elements. All mouse lines were backcrossed into the C57BL/6 genetic background for at least 12 generations. To generate embryos deficient in both *Apaf1* and *Bcl2l*, double heterozygous animals were interbred. The embryos were taken from timed matings and the day on which a vaginal plug was detected was assigned as E0.5.

### Histological analysis and immunohistochemistry

For histological analysis serial paraffin sections through the inner ear were stained with Hematoxylin and Eosin or Giemsa. Immunohistochemical detection of activated caspase 3 was performed with the rabbit anti-CM1 antibody as before (Cecconi et al., 1998). For Bcl-$X_L$ immunostaining with mouse anti-Bcl-$X_L$ (H-5) antibody (Santa Cruz), Bouin's-fixed paraffin sections were deparafinized and boiled for 20 minutes in 10 mM Citrate buffer (pH 6). After secondary antibody (donkey anti-mouse HRP IgG) treatment, the signal was amplified using the TSA Cyanine 3 System Kit (PerkinElmer Life Science Products). BrdU intraperitoneal injection and detection in proliferating cells were performed as before (Salminen et al., 2000). Anti-class III β-tubulin (TUJ1, Babco) was used as a control antibody. Three-dimensional reconstructions from histological sections of inner ears at stage E13.5 were constituted from serial paraffin cross-sections of 10 μm thickness. One ear from each genotype was used for reconstruction and the embryos all came from the same litter of a mating between two *Apaf1/Bcl2l* double heterozygous animals.

### RNA isolation and reverse transcription-polymerase chain reaction (RT-PCR) assay

Total RNA was isolated with Trizol Reagent (Life Technologies) from wild-type E9.5 and E11.5 mouse embryos. To detect the different splice variants produced from the *Bcl2l* gene, 2 μg of the isolated RNA was subjected to RT reaction using the RT-primer 5′-GACTGAAGAGTGAGCCCAGATC-3′. The forward and reverse primers for PCR were 5′-CAGTGAAGCAAGCGCTGAGAG-3′ and 5′-CGTCAGAAACCAGCGGTTGAAG-3′, respectively.

### RNA in situ hybridization and staining for β-galactosidase activity

In situ hybridization and preparation of the radioactive antisense and sense *Netrin1* (Serafini et al., 1996), *Pax2* (Dressler et al., 1990) and *Dlx5* (Acampora et al., 1999) probes were performed as described in Salminen et al. (Salminen et al., 2000). Whole-mount *lacZ* staining for E12.5 *Apaf1*$^{+/-}$ and $^{-/-}$ embryos was conducted as described in Hogan et al. (Hogan et al., 1994).

### Detection of apoptosis

Detection of apoptosis was performed with the in situ DNA-end labeling technique, the TUNEL method, that detects DNA fragmentation as an indicator of ongoing apoptosis. TUNEL analysis was performed on 10 μm-thick paraffin sections with the ApopTag Fluorescein In Situ Apoptosis Detection Kit (Intergen). The proportion of TUNEL-positive cells from all otic vesicle cells was calculated on serial sections of 2 or 3 E9.5, E10.5 or E12.5 embryos.

## Results

### Expression of *Apaf1* and *Bcl2l* genes during inner ear development

The expression of *Apaf1* and *Bcl2l* was analyzed at various stages during the early development. *Apaf1/lacZ* is widely expressed in developing embryos heterozygous for the *lacZ*-containing allele (Fig. 1L). A rather weak expression could be detected at E9.5-10.5 all through the otic vesicle and in the periotic mesenchyme developing into the otic capsule (Fig. 1A,B). At E12.5 highest levels of *Apaf1/lacZ* gene expression were observed in the

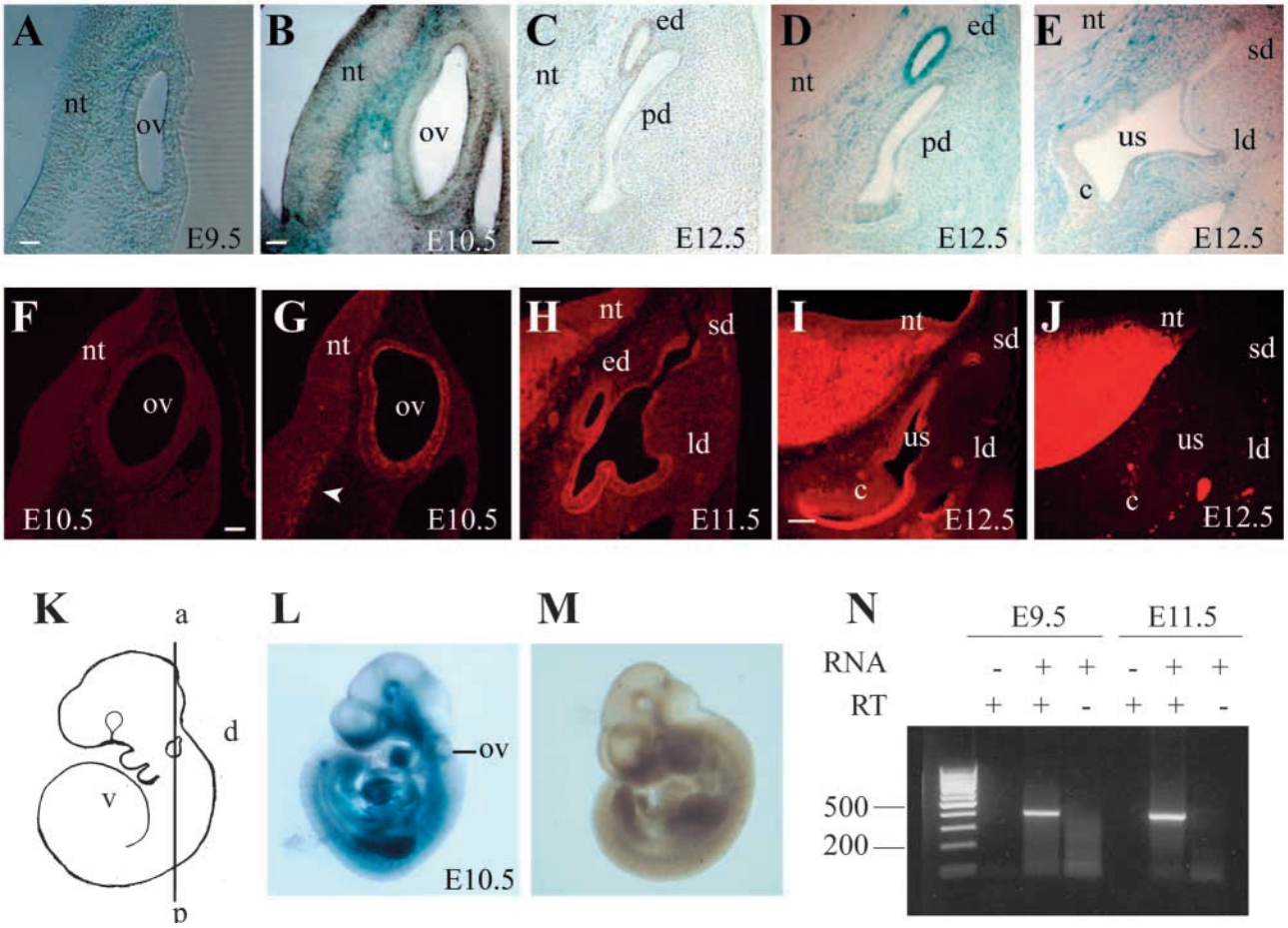


**Fig. 1.** Detection of Apaf1/*lacZ* and Bcl-$X_L$ in the developing inner ear at E12.5. *Apaf1/lacZ* expression could be detected in the otic epithelium and the surrounding mesenchyme at E9.5 (A), E10.5 (B) and E12.5 (D,E). No staining could be detected in sections from wild-type embryos (C). Bcl-$X_L$ protein could be detected in the otic epithelium but not in the periotic mesenchyme at E10.5 (G), E11.5 (H) and E12.5 (I). No staining in the otic region could be detected in control sections with only secondary antibody (F) or with TUJ1 antibody which specifically stains neurons (J). (K) Plane of the sections, (L) *lacZ* expression in a heterozygous *Apaf1*$^{+/-}$ embryo, (M) control staining in a wild-type embryo. (N) RT-PCR analysis of total RNA from E9.5 and E11.5 wild-type embryos. Only a 395 bp-long fragment corresponding to the Bcl-$X_L$ isoform was detected. Scale bar: 100 μm. a, anterior; c, cochlea; d, dorsal; ed, endolymphatic duct; ld, lateral semicircular duct; nt, neural tube; ov, otic vesicle; p, posterior; pd, posterior semicircular duct; sd, superior semicircular duct; us, utriculosaccular space; v, ventral.

endolymphatic duct epithelium. Expression could also be detected in the periotic mesenchyme and it was slightly elevated in the tips of the semicircular ducts as well as in the cochlear duct compared with the rest of the otic epithelium (Fig. 1D,E).

The *Bcl2l* gene has been shown to produce several protein isoforms through alternative splicing (Bcl-$X_S$) and cleavage of the major anti-apoptotic Bcl-$X_L$ isoform (Clem et al., 1998; Fujita et al., 1998). We detected the Bcl-$X_L$ isoform in the developing inner ear with an isoform-specific antibody and studied the expression of the alternatively spliced Bcl-$X_S$ isoform with RT-PCR assay. To our knowledge, antibodies specific for cleaved Bcl-$X_L$ protein isoforms are unavailable.

Bcl-$X_L$ immunoreactivity was found all over the otic epithelium at E10.5-12.5, but no protein could be detected in the periotic mesenchyme (Fig. 1G-I). To analyze the expression of the alternatively spliced Bcl-$X_S$ isoform we performed RT-PCR reactions on total RNA isolated from E9.5 and E11.5 otic vesicle and periotic mesenchyme. The RT-PCR primers were designed to hybridize to sequences common to both *Bcl-$X_L$* and *Bcl-$X_S$* so that *Bcl-$X_L$*-specific mRNA would give a 395 bp-long fragment and *Bcl-$X_S$*-specific mRNA a 206 bp-long fragment. As seen in Fig. 1N, only the *Bcl-$X_L$*-specific mRNA could be detected at E9.5 and E11.5.

### Changes in apoptotic profiles at E9.5-10.5 in the *Apaf1* and *Bcl2l* mutant inner ears

We compared the pattern of programmed cell death in *Apaf1* and *Bcl2l* mutant inner ears with the corresponding wild-type littermates. In an early otic vesicle, at E9.5-10.0, a TUNEL-positive cell cluster localized to the ventro-posterior area (arrowhead Fig. 2B) and a few scattered dying cells could be observed more dorsally. In *Apaf1* mutant otic vesicles, no apoptotic cells were detected at E9.5-10.5 (Fig. 2C and data not shown). In *Bcl2l* mutant otic epithelium, a significant 3-fold increase in the proportion of TUNEL-positive cells could be observed (Fig. 2D, Table 1).

Many TUNEL-positive cells were detected at the base of the wild-type endolymphatic duct at E10.5 (Fig. 2F). In the posterior part of the otic vesicle apoptotic cells were spread over a broad area extending dorsally (Fig. 2G). Anti-caspase 3

**Table 1. Increase in cell death in *Bcl2l* mutant otic epithelium**

| Stage | Wild type (%) | Bcl2l$^{-/-}$ (%) | *P* |
|---|---|---|---|
| E9.5 ov | 14.4±5.4 | 41.9±10.9 | <0.0001 |
| E10.5 ed | 25.5±11.3 | 77.2±8.8 | <0.0001 |
| E10.5 ov without ed | 16.9±6.5 | 29.9±5.9 | <0.0001 |
| E12.5 ssd | 25.8±6.7 | 52.0±8.6 | <0.0001 |

The proportion of TUNEL-positive cells from all otic vesicle cells was calculated on serial sections covering the whole vesicle at E9.5 or E10.5 (two embryos each genotype at each stage). In case of E10.5 the otic vesicle (ov) was divided in two areas: the endolymphatic duct (ed) and the rest of the epithelium. At E12.5, the proportion of TUNEL-positive cells was calculated in the tip of the outgrowing superior semicircular duct (ssd). The calculated mean values are given with standard deviation (±s.d.). The differences between wild-type and *Bcl2l* mutant values was analyzed using the two-tailed Student's *t*-test.

staining showed a very similar spatial pattern of dying cells to TUNEL (data not shown) but revealed far fewer cells. This discrepancy may be because of the fact that activated caspase 3 is present only transiently in dying cells, whereas the DNA breaks detected by the TUNEL assay persist for a longer period.

A marked 3-fold increase in the ratio of TUNEL-positive cells could be detected in the endolymphatic duct epithelium of the *Bcl2l* mutant embryos at E10.5 (Table 1). In addition, the distribution of dying cells in *Bcl2l* mutant ears extended more ventrally (Fig. 2H). In the rest of the otic vesicle, a 2-fold increase of TUNEL-positive cells could be observed (Table 1). A cluster of apoptotic cells could be observed in the ventro-posterior area of the *Bcl2l* mutant otic epithelium, but the broad area of apoptotic cells observed more dorsally in the wild-type otic vesicle (Fig. 2G) was not detected (Fig. 2H). Extensive cell movement occurs in the otic epithelium after its closure (Brigande et al., 2000) and thus, the lack of dying cells in the dorsal wall of the *Bcl2l* mutant otic vesicle could be because of premature death of these cells while still in a more ventro-posterior location (Fig. 2B,D).

Apoptosis has been thought to be responsible for the complete detachment of the mammalian otic vesicle from the surface ectoderm by removing the connecting epithelial stalk after the closure (Marovitz et al., 1976; Represa et al., 1990; Lang et al., 2000). We observed a cluster of apoptotic cells in the region between the surface ectoderm and the endolymphatic duct epithelium in wild-type embryos at E9.5 and E10.5 (Fig. 2F and data not shown). In the *Apaf1* mutant embryos (*n*=3), this apoptotic group of cells could not be observed but the otic vesicles had nevertheless closed normally (Fig. 2C). In *Bcl2l* mutant embryos (*n*=3) no clear cluster of apoptotic cells but instead a few scattered cells could be observed in the closure region (Fig. 2H).

Very little or no apoptosis could be observed in the periotic mesenchyme of the wild-type embryos (Fig. 2F,G). Apoptosis could, however, be detected elsewhere in the head mesenchyme (Fig. 2B,F). Also, no apoptosis could be observed in the periotic mesenchyme of either *Apaf1* or *Bcl2l* mutant embryos (Fig. 2C,D,H).

Taken together, our results demonstrate that the normal developmental apoptotic pattern had changed in both *Apaf1* and in *Bcl2l* mutant inner ears. The almost complete lack of apoptotic cells in the *Apaf1* mutant ears indicates that the majority of the apoptosis detected in the wild-type otic epithelium at E9.5-10.5 is Apaf1-dependent. Inactivation of the *Bcl2l* gene led to a general increase of cell death in the expected apoptotic areas of the otic epithelium. This result is probably because of the lack of the anti-apoptotic Bcl2l isoform. However, at the closure site, a decrease of apoptotic cell numbers was observed, suggesting that pro-apototic Bcl2l isoforms might be active there.

### Changes in the apoptotic pattern at E12.5

In wild-type embryos at E12.5, TUNEL-positive cells were detected in the endolymphatic duct epithelium (Fig. 3A), the wall of the cochlear duct (Fig. 3A-D), the distal edge of the three semicircular duct epithelium (shown for the superior duct in Fig. 3A-D, arrow in A) and the areas where the utricle, saccule and the cochlear duct will be separated by deepening

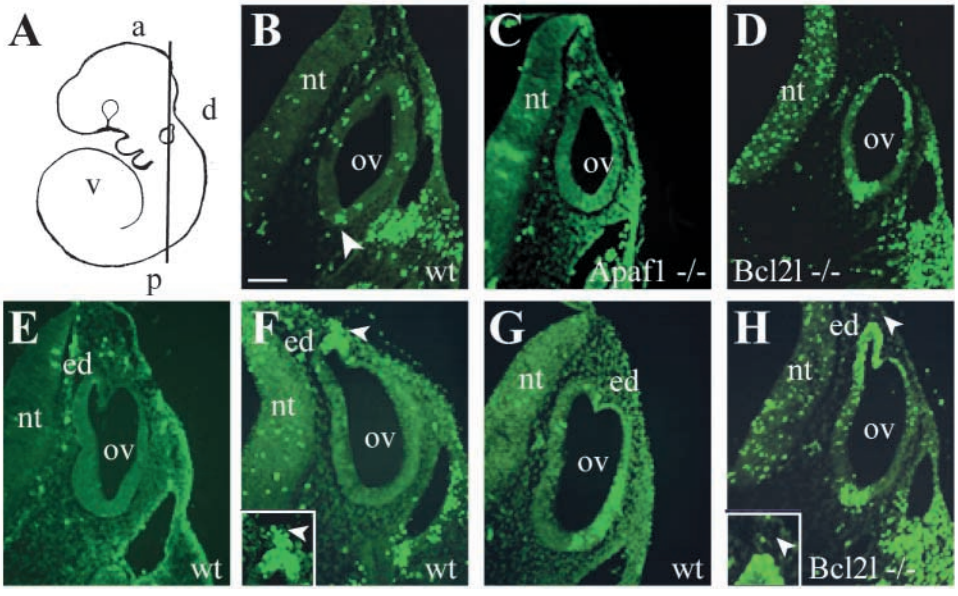


**Fig. 2.** Apoptosis during early otic vesicle development. (A) Plane of the sections. Dying cells were detected in cross-sections through the otic vesicle at E10.0 (B-D) and E10.5 (E-H) with the TUNEL method. (E) Negative control for TUNEL staining without terminal deoxynucleotidyl transferase. The genotypes of the embryos are indicated in each case. The arrowheads in F and H point to the dying cells observed between the otic vesicle and the surface ectoderm. A higher magnification of this area is shown in the left-hand corner in F and H. Scale bar: 50 μm.

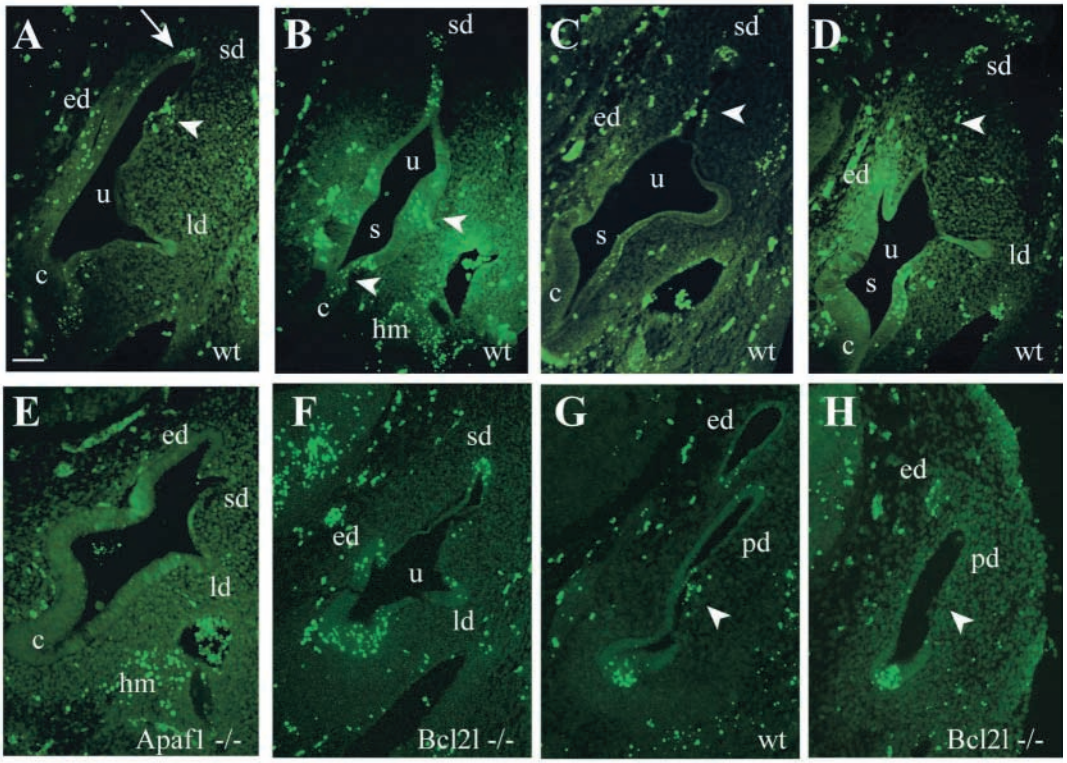


**Fig. 3.** Apoptosis in the inner ear at E12.5. TUNEL-positive cells in sections from wild-type (A-D,G), *Apaf1* (E) and *Bcl2l* mutant (F,H) embryos. The arrowheads in A, C and G point to TUNEL-positive cells at the future fusion plate-forming epithelium and the adjacent periotic mesenchyme. The arrowheads in B point to dying cells at the areas where the ducts separating the utricle, saccule and cochlear duct will become thinner. The arrow in A points to the TUNEL-positive cells at the outer edge of the semicircular duct. Scale bar: 100 μm. hm, head mesenchyme; s, saccule; u, utricle.

constrictions (Fig. 3B, arrowheads). In addition, some apoptotic cells were observed in the superior and posterior semicircular duct epithelium prior to the fusion in the area that is destined to form the fusion plate. A few dying cells were also detected in the immediately adjacent periotic mesenchyme (Fig. 3A,G, arrowheads). In accordance with previous observations (Martin and Swanson, 1993), we could not detect any dying cells when the two epithelial cell layers were opposed and fused (data not shown). However, a few TUNEL-positive cells were observed in the mesenchyme lining the small empty hole after the fusion plate had been cleared (arrowheads in Fig. 3C,D). In general, no or very little apoptosis occurred in other areas of the periotic mesenchyme at this stage.

Very few or no TUNEL-positive cells could be observed in the *Apaf1* mutant ($n$=6) otic epithelium or the periotic mesenchyme. Further away from the ear, in the head mesenchyme, apoptosis could, however, be detected as in the wild-type embryos, suggesting an Apaf1-independent mechanism for the removal of these cells (Fig. 3E). In the *Bcl2l* mutant ($n$=6) ears, an overall increase of TUNEL-labeled cells could be detected in the normal locations of the otic epithelium (Fig. 3F). In the tips of the outgrowing superior semicircular duct a 2-fold increase was observed (Table 1). However, a local lack of apoptosis could be observed in the future fusion plate epithelium and the adjacent periotic mesenchyme of the posterior semicircular duct as compared with the wild-type embryos (compare Fig. 3G,H, arrowheads). No TUNEL-positive cells could be detected in the *Bcl2l* mutant periotic mesenchyme (Fig. 3F,H).

In summary, our results suggest that very little or no Apaf1-independent apoptosis occurs in the otic epithelium at E12.5. In the *Bcl2l* mutant embryos a general increase of apoptosis was observed as at earlier stages, except for the fusion plate area of the posterior semicircular duct where a lack of apoptotic cells was observed. Very little apoptosis can be detected in the periotic mesenchyme, suggesting that apoptosis is not critical for the formation of the otic capsule.

### Three-dimensional reconstructions of the mutant inner ears reveal specific morphogenetic defects and reduced growth

The morphogenetic architecture of the membranous labyrinth has been established by E13.5. To examine the morphology of the epithelial labyrinths of the embryos at this stage we reconstructed three-dimensional images from serial sections. The reconstructions showed that both *Apaf1* and *Bcl2l* mutant ears were smaller than the wild-type ears and were reduced to 54% and 70%, respectively (Fig. 4A-C). The diameter of the corresponding mutant heads were 86% and 77% of that of the wild-type heads, respectively (data not shown), which could explain the reduction in membranous labyrinth size in the case of *Bcl2l* mutants but not in the case of *Apaf1* mutants.

The lack of apoptosis in the *Apaf1* mutant inner ear epithelium led to severe abnormalities in morphogenesis (Fig. 4B). The inner ear epithelium appeared misshapen and there were no clear borders between the different compartments. The endolymphatic duct was not properly elongated and instead, an enlarged sac-like structure could be seen. At later stages (E16.5-18.5), dorsal extension of the endolymphatic duct could be observed, but the diameter of the duct always remains larger than in the wild-type embryos, and therefore no sac structure could be distinguished (Fig. 5A-C and data not shown). The two semicircular duct outpocketings that form first, the superior and posterior, show a small clearing of the fusion plate at E13.5 as seen also in Fig. 4E for the posterior duct. At this stage, the lateral semicircular duct remained as a very small outpocketing without visible cleared area in the middle. The

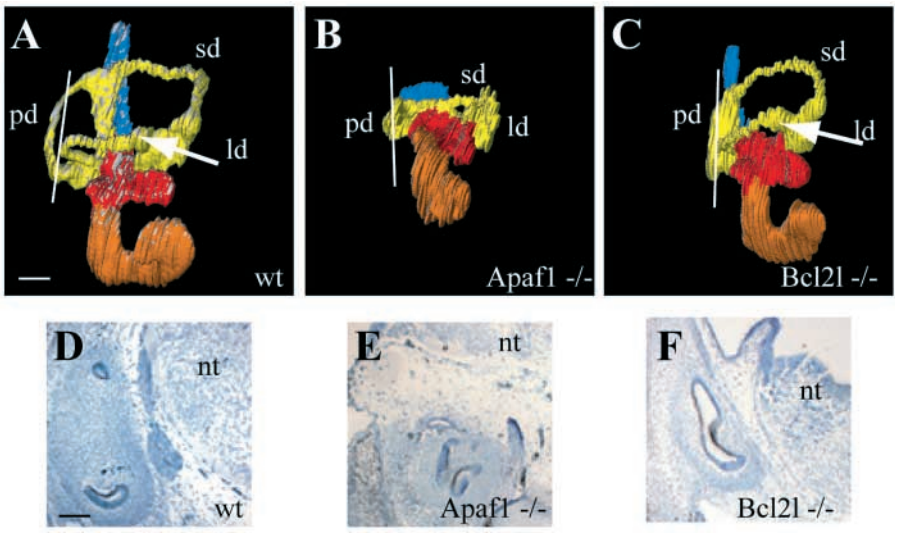


**Fig. 4.** Three-dimensional reconstructions of the inner ear epithelium at E13.5. Otic epithelium was reconstructed from serial sections through wild-type (A), *Apaf1* (B) and *Bcl2l* (C) mutant inner ears. All three embryos came from the same double heterozygous mating. A lateral view is shown, dorsal is up, ventral down. The *Apaf1* ear has been turned so that it corresponds to the two others. Endolymphatic duct is indicated with a blue color, the semicircular ducts with yellow, the utricle and saccule with red and the cochlea with an orange color. The white line shows the plane of the section through the posterior duct shown in D-F. The black dots indicate *Netrin1* expression after RNA in situ hybridization in D-F. Scale bars: 60 μm in A-C; 100 μm in D-F.

cochlear duct was much shorter and more immature in shape compared with the wild-type duct.

The morphology of the *Bcl2l* mutant inner ear was rather normal except for the posterior semicircular duct that does not form at all. Instead, an outpocketing without epithelial fusion or clearing in the middle could be observed (Fig. 4C,F). In all nine *Bcl2l* mutant embryos analyzed at E13.0-13.5 the posterior duct failed to form.

The three-dimensional reconstructions demonstrated that the decrease of apoptosis in *Apaf1* mutant embryos led to a growth retardation and to defects in shaping or 'sculpting' the membranous labyrinth. *Bcl2l* inactivation led only to a restricted phenotype concerning the posterior semicircular duct.

## Superior semicircular duct formation is most severely affected in *Apaf1* mutant embryos

Some variation in the severity of the phenotype of the *Apaf1* mutant ears could be observed when sections through the ears of 16 E12.5-18.5 embryos were analyzed. General variability in *Apaf1* mutant phenotypes has been observed before. In the case of brain, variation ranges from severely overgrown nervous tissue to a completely normal-looking tissue (Cecconi et al., 1998; Honarpour et al., 2000). We obtained embryos at a ratio of 10/6 for severe/mild phenotypes judged according to the brain overgrowth. The severity of the inner ear morphological phenotype seemed to correlate to some extent with that in the brain. The *Apaf1* mutant inner ear in Fig. 4B,E comes from an embryo with a highly overgrown and open brain structure, whereas Fig. 5B,C shows the two ears from an embryo with no obvious brain defects. In embryos in which brain overgrowth was extensive, the ear was often aberrantly positioned directly ventrally from the neural tube instead of its normal lateral position (Fig. 4E). In addition, the ear had turned in a more horizontal position. However, irrespective of the severity of the brain phenotype or ear position, the inner ear epithelium was always reduced except for the endolymphatic duct which was always enlarged (Fig. 4B, Fig. 5B,C). In addition, the superior semicircular duct was always markedly reduced (Fig. 5B) and sometimes completely absent (41%) even in embryos with no detectable brain phenotype (asterisk in Fig. 5C). The other two semicircular ducts always formed and a

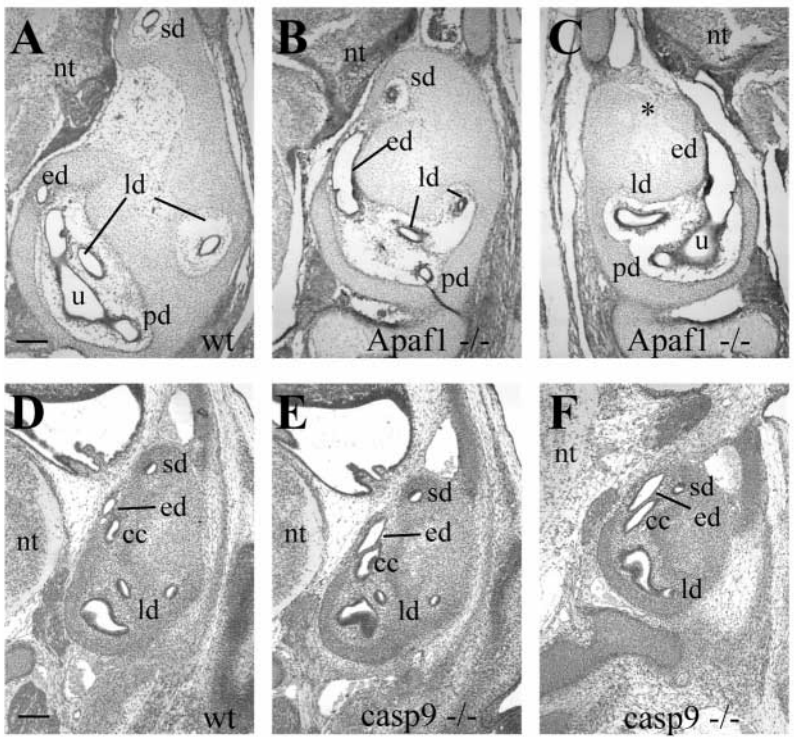


**Fig. 5.** Variability in *Apaf1* and caspase 9 inner ear phenotype. Cross-sections through the inner ear at E16.5 (A-C) and E13.5 (D-F). The images in B and C show sections from the two ears from the same *Apaf1* mutant embryo with no brain phenotype. The lack of superior semicircular duct is indicated with an asterisk in C. The section in E comes from a caspase 9 mutant embryo with a mild brain phenotype, and in F from an embryo with a severe brain phenotype. Scale bar: 100 μm. cc, crus commune.

clearing of the fusion plates could be detected by E14.5 (Fig. 4E, Fig. 5B,C).

The periotic mesenchyme seems to develop normally as judged from those *Apaf1* mutant embryos that lived until E16.5-18.5 (*n*=5). The mesenchymal cells closest to the otic epithelium are destined to undergo cell death once the main morphogenetic events have occurred to generate the perilymphatic space between the membranous and bony labyrinths. Interestingly, this late cell death seems to occur normally in the absence of Apaf1 (Fig. 5A-C).

### The inner ear phenotype in the caspase 9 mutant embryos closely resembled that of *Apaf1* mutants

The results from the analyses of *Apaf1* mutant animals emphasized the importance of Apaf1 for the developmental apoptosis that occurs during otic epithelium morphogenesis. To determine whether this cell death involves the apoptosome or occurs through an apoptosome-independent pathway (Marsden et al., 2002), we analyzed the inner ear phenotype in six caspase 9 mutant embryos at E13.5-17.5.

The inner ear phenotype in caspase 9 mutant embryos including morphogenetic changes (enlarged endolymphatic duct), smaller size, reduced semicircular ducts and variation in phenotype severity was very similar to that observed in *Apaf1* mutant embryos (Fig. 5D-F and data not shown). As for other organs affected, the caspase 9 phenotype appeared slightly milder than the *Apaf1* phenotype (Cecconi et al., 1998; Yoshida et al., 1998; Kuida et al., 1998; Hakem et al., 1998). These results support the idea that most of the cell death in the developing inner ear occurs through the activation of the apoptosome complex.

### Dorso-ventral compartmentalization occurred normally in *Apaf1* and *Bcl2l* mutant otic epithelium

To verify whether the regionalization of the inner ear epithelium occurred normally in *Apaf1* and *Bcl2l* mutant inner ears, we performed in situ hybridization analyses with marker genes known to be specific for either dorsal or ventral parts of the inner ear. The *Dlx5* gene was expressed normally in the dorsal vestibular part and in the endolymphatic duct of both mutants (shown for wild-type and *Apaf1* mutant in Fig. 6A,B). *Pax2* expression was detected ventrally along the utricular wall and in the developing cochlear duct (shown for wild-type and *Bcl2l* mutant in Fig. 6C,D). *Netrin1* is specifically expressed in the semicircular duct fusion-plate-forming epithelium and after duct formation it remains expressed at the inner edge of the duct epithelium (Salminen et al., 2000). In both *Apaf1* and *Bcl2l* mutant ears *Netrin1* was expressed in the fusion plate-forming cells as well as the newly formed ducts (Fig. 4D-F, Fig. 6E-F). These results demonstrate that in spite of the changes in apoptotic patterns, abnormal cell positional identities could not be detected in the mutants.

### Cell proliferation changes in *Apaf1* and *Bcl2l* mutant otic epithelium

In many cases, the *Apaf1* membranous labyrinth was reduced to almost half of the normal size at E13.5 (Fig. 4A,B). To verify whether cell proliferation was affected to the same extent in different parts of the epithelium, we performed BrdU injections into pregnant females and stained sections from the obtained embryos with an anti-BrdU antibody. We chose to analyze two

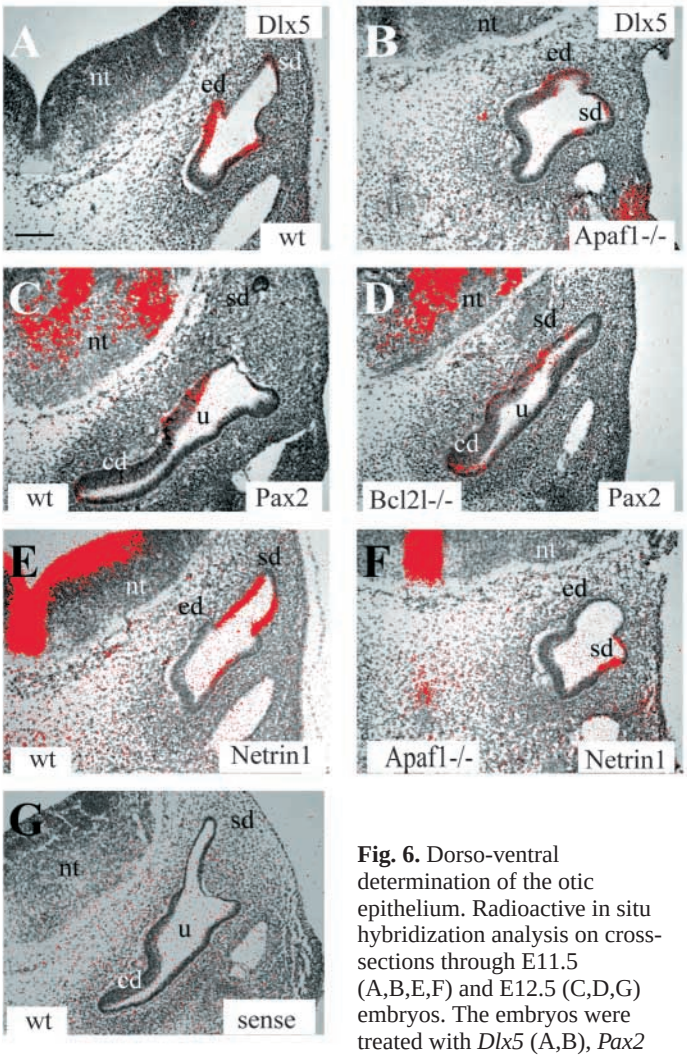


**Fig. 6.** Dorso-ventral determination of the otic epithelium. Radioactive in situ hybridization analysis on cross-sections through E11.5 (A,B,E,F) and E12.5 (C,D,G) embryos. The embryos were treated with *Dlx5* (A,B), *Pax2* (C,D) and *Netrin1* (E,F) antisense probes and with *Netrin1* sense probe (G). Scale bar: 100 μm.

stages, E11.5 and E12.5, in which the epithelial outgrowth is most active. To calculate the proliferation indexes we analyzed sections from two wild-type and two mutant embryos at each stage.

In the severely affected *Apaf1* mutant embryos, the overall size of the otic epithelium was clearly diminished already at E11.5 (Fig. 7A,B). In these ears, 22.9%±5.5% of the cells were proliferating in comparison with the wild-type ears in which the proliferation index was 33.4%±4.9% ($P$<0.001, Student's *t*-test). At E12.5 the defect in the semicircular duct outgrowth became evident (compare superior and lateral ducts in Fig. 7F,G). However, no clear difference in the proliferation index could no longer be detected here (data not shown). The consequence of a decrease in the proliferation index at an earlier stage could be observed as a strong reduction in the number of cells in the mutant duct area at later stages. At E12.5 the proliferation index in the cochlear duct was 40.4%±10.3% in the *Apaf1* mutant and 68.8%±13.6% ($P$<0.001) in the wild-type (examples in Fig. 7G,H). Moreover, an almost complete lack of proliferating cells was observed in the outer wall of the turning cochlear duct (arrowheads in Fig. 7G,H). No clear

change in the local cell proliferation could be observed in the endolymphatic duct epithelium between wild-type and *Apaf1* mutant embryos at E11.5 (data not shown).

Interestingly, the dramatic increase of apoptosis in the otic epithelium of the *Bcl2l* mutant embryos did not seem to have much of an effect on its final size at E13.5, suggesting that the increased apoptosis stimulated a compensatory increase in cell proliferation. To verify this we compared cell proliferation in wild-type (46.1%±10.2%) and *Bcl2l* mutant otic vesicles (55.7%±9.3%) at E10.5 and observed a significant increase in proliferation ($P$<0.0001) in *Bcl2l* mutant inner ears (examples in Fig. 7D,E). At this stage, no clear difference (p=0.42) in the total number of otic epithelium cells could be observed between wild-type (189.7±19.7 average number of cells/section±s.d.) and *Bcl2l* mutant (184.5±15.5) embryos ($n$=2). At later stages, no significant difference could be observed in proliferation indexes, for example, in the tips of the outgrowing semicircular ducts (data not shown). At E13.5 the mutant semicircular ducts appeared slightly thinner (Fig. 4A,C) and the number of cells (24.6±3.1) in cross-sections through the superior duct of the *Bcl2l* mutant ears ($n$=2) was 26% smaller than in wild-type ones (33.2±3.9, $P$<0.0001).

Taken together, our results suggest that Apaf1-dependent apoptosis might be required to achieve the normal level of cell proliferation in the developing otic epithelium excluding the area of the endolymphatic duct. Lack of apoptosis seemed to especially affect the outgrowth of the semicircular and the cochlear ducts. Furthermore, an increase in apoptosis in *Bcl2l* mutant inner ears seems to result in an increase of proliferation at early stages that could at least partially compensate for the important loss of cells through excess cell death.

### Otic vesicle closure failed to occur in *Apaf1/Bcl2l* double mutant mice

In order to check whether the anti-apoptotic Bcl2l and the pro-apototic Apaf1 operated independently of each other or through a common pathway during inner ear development, we generated double mutant embryos. These embryos died at E12.5-13.0, similar to the *Bcl2l* single mutants, and suffered from a hematopoietic failure indicating that the inactivation of *Apaf1* cannot inhibit the excessive cell death occurring in the hematopoietic system when the *Bcl2l* gene is inactivated (Motoyama et al., 1995). Apaf1 deficiency did, however, prevent the increased cell death observed in immature neurons throughout the embryonic Bcl2l-deficient nervous system (Motoyama et al., 1995) (data not shown). The same observations have been reported by Yoshida et al. (Yoshida et al., 2002).

We analyzed the inner ear phenotype in three double mutant embryos at E11.5. In none of the three cases did the otic epithelium undergo massive apoptosis as in *Bcl2l* mutants. Instead, no apoptosis could be detected, a phenotype very similar to that of *Apaf1* mutant inner ears (Fig. 8A-B). This result suggests that in contrast to the hematopoietic system, the excess of cell death that results from *Bcl2l* inactivation requires Apaf1 in the inner ear.

The epithelial morphogenesis of the inner ear in the double mutant embryos occurred in a very similar way to that in *Apaf1* mutants. However, the otic vesicle failed to close completely in all the six mutant ears that were analyzed (Fig. 8B,D, arrows). The imperfect closure may have led to the lack of any morphologically detectable endolymphatic duct formation, because normally the endolymphatic duct forms close to the site where the closure has taken place. In other areas of the otic vesicle the regionalization occurred normally and *Netrin1*, *Dlx5* and *Pax2* expression could be detected in anticipated areas (Fig. 8F-G and data not shown).

## Discussion

### Programmed cell death is required to shape the membranous labyrinth

In *Apaf1* mutant embryos, none or very few dying cells could be observed in the otic epithelium leading to a malformed membranous labyrinth in which different compartments were not clearly defined. In addition, the endolymphatic duct remained enlarged and no sac structure could be distinguished. Therefore, the localized Apaf1-dependent apoptosis that normally removes cells at the constriction sites and at the base of the endolymphatic duct is required for the correct shaping

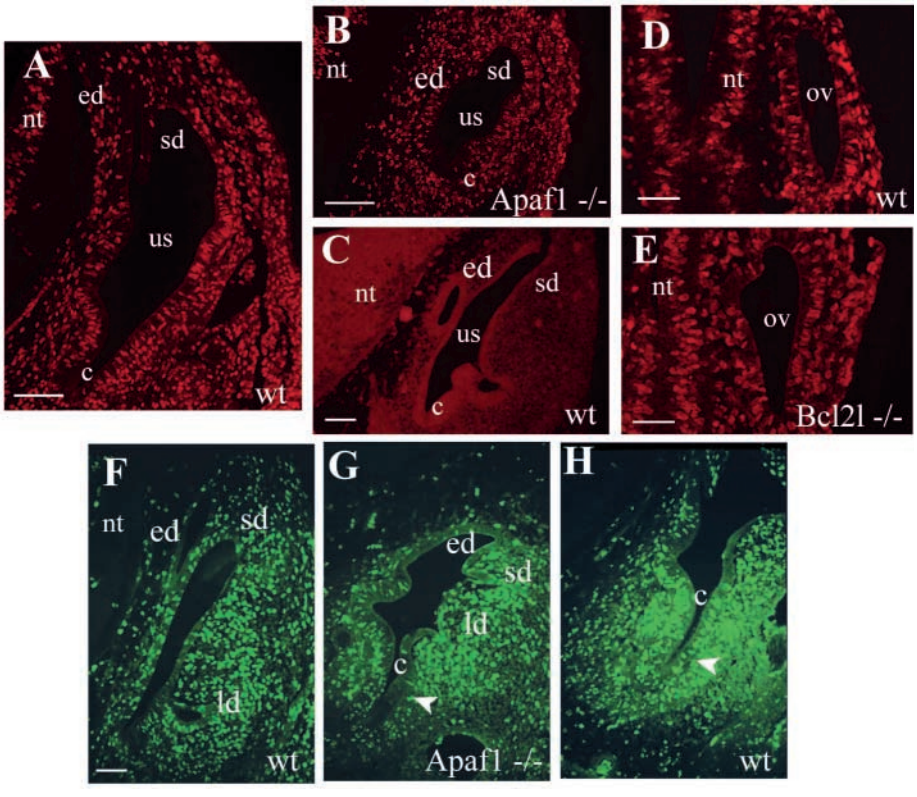


**Fig. 7.** Cell proliferation in *Apaf1* and *Bcl2l* mutant otic epithelium. Proliferating cells were detected with an anti-BrdU antibody staining of the developing inner ear at E11.5 (A-C), at E10.5 (D-E) and E12.5 (F-H) in wild-type (A,D,F,H), *Apaf1* (B,G) and *Bcl2l* (E) mutant otic epithelium. Control staining with secondary antibody only (C). Scale bar: 100 μm.

of the organ. The inner ear phenotype of the caspase 9 mutant embryos closely resembled that of *Apaf1* mutants, strongly suggesting that Apaf1 affects inner ear morphogenesis through the apoptosome complex.

The morphogenesis of the three semicircular ducts is a complex procedure, the main steps of which seem to be common for all of them. However, targeted mutations of several genes in mouse have shown selective defects in duct formation and suggested that the formation of each duct might be independently controlled by specific sets of genes (Fekete, 1999). Here we show that the inactivation of the *Bcl2l* gene selectively affects the formation of the posterior semicircular duct. This phenotype could be because of the observed lack of local apoptosis at the fusion plate-forming epithelium and/or in the adjacent periotic mesenchyme, suggesting that pro-apoptotic Bcl2l isoforms may have a developmental role there. Fekete et al. (Fekete et al., 1997) have shown that overexpression of the *Bcl2* gene in chicken embryos leads to a block of cell death that most severely affects the posterior duct. These observations suggest a special regulatory role for Bcl2 family members concerning the development of the posterior duct of the two species. Interestingly, Apaf1 also seems to be required especially for one of the semicircular ducts; the growth of the superior duct is most severely affected in *Apaf1* mutant embryos.

Some variation of the *Apaf1* mutant inner ear development was observed and the severity of the phenotype correlated with that observed in the brain. Therefore, it is possible that a severely overgrown hindbrain enhances the aberrant ear phenotype. However, we observed that the principal structural and growth defects were present also in *Apaf1* mutant embryos where no brain phenotype could be detected.

## Apoptosis and outgrowth of the inner ear epithelium

Unneeded cells are removed by apoptosis in many organs during development. The phenomenon is most striking in brain where in some areas nearly 50% of the cells are eliminated (reviewed by D'Mello, 1998). In *Apaf1* mutant mice, there is a decrease in apoptosis in many neuronal populations including neural precursors. This results in an increased amount of cells undergoing cell division and to overgrowth of the brain mass (Cecconi et al., 1998; Yoshida et al., 1998).

A balance between cell proliferation and apoptosis also seems to play a critical role during inner ear development. There are regional differences in the proliferative activity in the otic vesicle resulting in differential outgrowth of the epithelium (Lang et al., 2000). In some areas where cells undergo active proliferation, dying cells are abundant. These areas include the distal edges of the semicircular ducts and the wall of the cochlear duct (Fekete et al., 1997; Nicolic et al., 2000). In *Apaf1* mutant embryos, a surprising size reduction of the membranous labyrinth was already observed at E11.5 and cell proliferation had diminished by 10-30% depending on the area and stage analyzed. There was an especially clear reduction in the elongation of the cochlear duct and the outgrowth of the semicircular ducts. Therefore, the morphogenetic defects observed in the cochlea and in the semicircular ducts seem to be a consequence of decreased proliferation together with decreased apoptosis.

How does the lack of apoptosis affect cell proliferation in these outgrowing areas of the otic epithelium? Apoptosis might stimulate proliferation through increasing locally the amount of growth-promoting factors released to the environment. This kind of passive release of functional factors into the environment from dying cells has been described (Scaffidi et al., 2002). Fibroblast growth factors (FGFs) are potential candidates to promote otic growth because several of them are expressed in the otic epithelium during its outgrowth period (reviewed by Noramly and Graigner, 2002). Interestingly, a subset of extracellular FGFs do not have any signal peptide and it has been proposed that they could be released passively from damaged cells (reviewed by Ornitz and Itoh, 2001).

In *Bcl2l* mutant inner ears a dramatic increase of apoptosis was observed at certain locations at E9.5-10.5. The excess of cell death seems to be at some extent compensated by an increase in cell proliferation because the ear is not smaller than in the wild-type littermates at this early stage. In mice with a

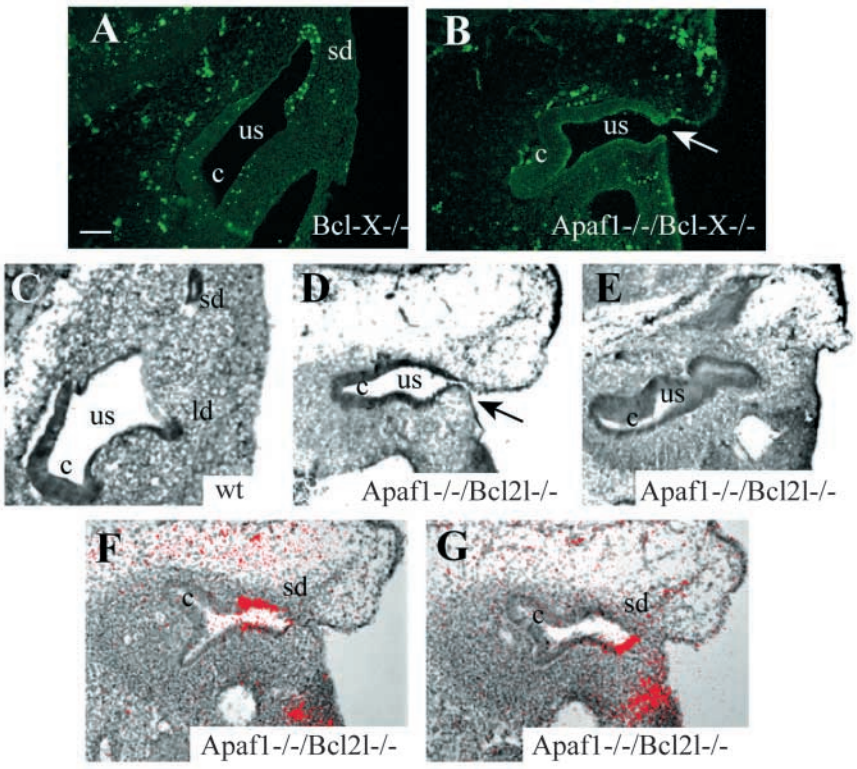


**Fig. 8.** Analysis of the inner ear in *Apaf1*$^{-/-}$/*Bcl2l*$^{-/-}$ double mutant embryos. Many TUNEL-positive cells could be observed in the otic epithelium of *Bcl2l*$^{-/-}$ embryos (A) at E11.5. No apoptosis could be observed in the *Apaf1*$^{-/-}$/*Bcl2l*$^{-/-}$ double mutant otic epithelium (B). In the wild-type embryo, the superior semicircular duct has already formed (C), whereas more immature morphogenesis can be observed in the *Apaf1*$^{-/-}$/*Bcl2l*$^{-/-}$ double mutant otic epithelium (D-E). The arrows in B and D point to the closure defect in the double mutant otic vesicles. In situ hybridization analysis shows *Dlx5* (F) and *Netrin1* (G) expression in the double mutant superior semicircular duct outpocketing. Scale bar: 100 μm.

targeted mutation in the *Bcl2* gene an increase in apoptosis can be observed during development of many organs. This leads to a dramatic decrease in the overall size of some organs such as spleen, kidney and thymus. However, some cell types in the developing kidney, such as the epithelium and interstitium, hyperproliferated, leading to increased numbers of these cell types (Veis et al., 1993). Thus, it seems that in some organs and cell types increased apoptosis may lead to overproliferation and decreased apoptosis to a growth delay.

More direct molecular links between proliferation and cell death have been proposed in several cell culture studies involving caspases (reviewed by Guo and Hay, 1999; Los et al., 2001; Mendelsohn et al., 2002) and Bcl2 family members (Los et al., 2001). How Apaf1 and apoptosis affect cell proliferation in the otic epithelium remains to be clarified. Another open question is why the phenotypes in brain and ear are so different. It may be because of the fact that the neuroectodermal cells continue to proliferate by default in the absence of cell death, whereas the ectodermal cells of placodal origin do not seem to proliferate by default and might require stimuli and signals from the neighboring dying cells in order to proliferate normally.

### Closure of the otic vesicle does not occur in the absence of both *Apaf1* and *Bcl2l* gene products

Apoptotic cells have been detected in the area of otic vesicle closure in normal embryos. However, no defects related to the closure were observed in *Apaf1* or *Bcl2l* single mutant embryos. Interestingly, when *Apaf1* mutation was introduced into the *Bcl2l*-deficient background, the otic vesicle closure was incomplete in 100% of the mutants. These observations suggest that *Apaf1* and pro-apoptotic *Bcl2l* gene product(s) may have redundant functions in controlling cell death at the closure site. The function of pro-apoptotic *Bcl2l* gene product(s) at the otic vesicle closure site is further supported by the fact that we observed a reduction, rather than an increase, in cell death at the otic vesicle closure site in *Bcl2l* mutant embryos. The *Apaf1*$^{-/-}$/*Bcl2l*$^{-/-}$ phenotype is the first example of an otic vesicle closure defect in mouse mutants. Interestingly, the otic epithelium compartmentalization seems to occur despite its incomplete closure.

In conclusion, we show that Apaf1-dependent and Bcl-$X_L$-regulated apoptosis is critical for the normal morphological development and the outgrowth of the otic epithelium. Furthermore, we propose that, together with Apaf1, pro-apoptotic Bcl-$X_L$ isoform(s) produced from cleavage of Bcl-$X_L$ could play a role in otic vesicle closure and in the formation of the posterior semicircular duct.

We thank Giovanni Levi and Marc Tessier-Lavigne for the probes, and Richard Flavell for caspase 9 mutant mice. We are grateful to Luydmula Rasskazova, Christel Pussinen, Mariana Loto, Cecelia Latham and Barbara Klocke for expert technical assistance. We also thank Irma Thesleff and Juha Partanen for helpful suggestions during the preparation of the manuscript. This work was funded by the Finnish Academy, the Sigrid Jusélius Foundation, the Biocentrum Helsinki Organization, the Max Planck Society, EMBO, NIH (NS35107) and Telethon Italy (grant TCP99038).

## References

**Acampora, D., Merlo, G. R., Paleari, L., Zerega, B., Postiglione, M., Mantero, S., Bober, E., Barbieri, O., Simeone, A. and Levi, G.** (1999). Craniofacial, vestibular and bone defects in mice lacking the Distal-less-related gene Dlx5. *Development* **126**, 3795-3809.

**Basañez, G., Zhang, J., Chau, B. N., Maksaev, G. I., Frolov, V.A., Brandt, T. A., Burch, J., Hardwick, J. M. and Zimmerberg, J.** (2001). Pro-apoptotic cleavage products of Bcl-xL form cytochrome c-conducting pores in pure lipid membranes. *J. Biol. Chem.* **276**, 31083-31091.

**Brigande, J. V., Iten, L. E. and Fekete, D. M.** (2000). A fate map of chick otic cup closure reveals lineage boundaries in the dorsal otocyst. *Dev. Biol.* **227**, 256-270.

**Cecconi, F., Alvarez-Bolado, G., Meyer, B. I., Roth, K. and Gruss, P.** (1998). Apaf1 (CED-4 homolog) regulates programmed cell death in mammalian development. *Cell* **94**, 727-737.

**Cecconi, F. and Gruss, P.** (2001). Apaf1 in developmental apoptosis and cancer: how many ways to die? *Cell. Mol. Life Sci.* **58**, 1688-1697.

**Clem, R. J., Cheng, E. H., Karp, C. L., Kirsch, D. G, Ueno, K., Takahashi, A., Kastan, M. B., Griffin, D. E., Earnshaw, W. C., Veliuona, M. A. et al.** (1998). Modulation of cell death by Bcl-XL through caspase interaction. *Proc. Natl. Acad. Sci. USA* **95**, 554-559.

**Dressler, G. R., Deutsch, U., Chowdhury, K., Nornes, H. O. and Gruss, P.** (1990). Pax2, a new murine paired-box-containing gene and its expression in the developing excretory system. *Development* **109**, 787-795.

**D'Mello, S. R.** (1998). Molecular regulation of neuronal apoptosis. In *Current Topics in Developmental Biology*, Vol. 39 (ed. R. A. Pedersen and G. P. Schatten), pp. 187-213. London: Academic Press.

**Fekete, D. M.** (1999). Development of the vertebrate ear: insights from knockouts and mutants. *Trends Neurosci*. **22**, 263-269.

**Fekete, D. M., Homburger, S. A., Waring, T., Riedl, A. E. and Garcia, L. F.** (1997). Involvement of programmed cell death in morphogenesis of the vertebrate inner ear. *Development* **124**, 2451-2461.

**Fujita, N., Nagahashi, A., Nagashima, K., Rokudai, S. and Tsuruo, T.** (1998). Acceleration of apoptotic cell death after the cleavage of Bcl-XL protein by caspase-3-like proteases. *Oncogene* **17**, 1295-1304.

**Guo, M. and Hay, B. A.** (1999). Cell proliferation and apoptosis. *Curr. Opin. Cell Biol.* **11**, 745-752.

**Hakem, R., Hakem, A., Duncan, G. S., Henderson, J. T., Woo, M., Soengas, M. S., Elia, A., de la Pompa, J. L., Kagi, D., Khoo, W. et al.** (1998). Differential requirement for caspase 9 in apoptotic pathways in vivo. *Cell* **94**, 339-352.

**Hogan, B., Beddington, R., Constantini, F. and Lacy, E.** (1994). *Manipulating The Mouse Embryo*. Cold Spring Harbor, NY: Cold Spring Harbor Laboratory Press.

**Honarpour, N., Du, C., Richardson, J. A., Hammer, R. E., Wang, X. and Herz, J.** (2000). Adult Apaf-1-deficient mice exhibit male infertility. *Dev. Biol.* **218**, 248-258.

**Kluck, R. M., Bossy-Wetzel, E., Green, D. R. and Newmeyer, D. D.** (1997). The release of cytochrome c from mitochondria: a primary site for Bcl-2 regulation of apoptosis. *Science* **275**, 1132-1136.

**Kuida, K., Haydar, T. F., Kuan, C. Y., Gu, Y., Taya, C., Karasuyama, H., Su, M. S. and Flavell, R. A.** (1998). Reduced apoptosis and cytochrome c-mediated caspase activity in mice lacking caspase 9. *Cell* **94**, 325-337.

**Lang, H., Miller Bever, M. and Fekete, D. M.** (2000). Cell proliferation and cell death in the developing chick inner ear: spatial and temporal patterns. *J. Comp. Neurol.* **417**, 205-220.

**Los, M., Stroh, C., Janicke, R. U., Engels, I. H. and Schulze-Osthoff, K.** (2001). Caspases: more than just killers? *Trends Immunol.* **22**, 31-34.

**Marovitz, W. F., Shugar, J. M. and Khan, K. M.** (1976). The role of cellular degeneration in the normal development of (rat) otocyst. *Laryngoscope* **86**, 1413-1425.

**Marovitz, W. F., Khan, K. M. and Schulte, T.** (1977). Ultrastructural development of the early rat otocyst. *Ann. Otol. Rhinol. Laryngol. Suppl.* **86**, 9-28.

**Marsden, V. S., O'Connor, L., O'Reilly, L. A., Silke, J., Metcalf, D., Ekert, P. G., Huang, D. C. S., Cecconi, F., Kuida, K., Tomaselli, K. J. et al.** (2002). Apoptosis initiated by Bcl-2-regulated caspase activation independently of the cytochrome c/Apaf-1/caspase-9 apoptosome. *Nature* **419**, 634-637.

**Martin, P. and Swanson, G. J.** (1993). Descriptive and experimental analysis of the epithelial remodellings that control semicircular canal formation in the developing mouse inner ear. *Dev. Biol.* **159**, 549-558.

**Mendelsohn, A. R., Hamer, J. D., Wang, Z. B. and Brent, R.** (2002). Cyclin D3 activates Caspase 2, connecting cell proliferation with cell death. *Proc. Natl. Acad. Sci. USA* **99**, 6871-6876.

**Motoyama, N., Wang, F., Roth, K., Sawa, H., Nakayama, K., Nakayama,**

**K., Negishi, I., Senju, S., Zhang, Q., Fujii, S. et al.** (1995). Massive cell death of immature hematopoietic cells and neurons in Bcl-x-deficient mice. *Science* **267**, 1506-1510.

**Nicolic, P., Järlebark, L. E., Billet, T. and Thorne, P. R.** (2000). Apoptosis in the developing rat cochlea and its related structures. *Dev. Brain Res.* **119**, 75-83.

**Nishikori, T., Hatta, T., Kawauchi, H. and Otani, H.** (1999). Apoptosis during inner ear development in human and mouse embryos: an analysis by computer-assisted three-dimensional reconstruction. *Anat. Embryol.* **200**, 19-26.

**Noramly, S. and Grainger, R. M.** (2002). Determination of the embryonic inner ear. *J. Neurobiol.* **53**, 100-128.

**Ornitz, D. M. and Itoh, N.** (2001). Fibroblast growth factors. *Genome Biol.* **2**, 3005.1-3005.12.

**Represa, J. J., Moro, J. A., Pastor, F., Gato, A. and Barbosa, E.** (1990). Patterns of epithelial cell death during early development of the human inner ear. *Ann. Otol. Rhinol. Laryngol.* **99**, 482-488.

**Salminen, M., Meyer, B. I. and Gruss, P.** (1998). Efficient polyA trap approach allows the capture of genes specifically active in differentiated embryonic stem cells and in mouse embryos. *Dev. Dyn.* **212**, 326-333.

**Salminen, M., Meyer, B. I., Bober, E. and Gruss, P.** (2000). Netrin 1 is required for semicircular canal formation in the mouse inner ear. *Development* **127**, 13-22.

**Sanders, E. J. and Wride, M. A.** (1995). Programmed cell death in development. *Int. J. Cytol.* **163**, 105-173.

**Scaffidi, P., Misteli, T. and Bianchi, M. E.** (2002). Release of chromatin protein HMGB1 by necrotic cells triggers inflammation. *Nature* **418**, 191-195.

**Serafini, T., Colamarino, S. A., Leonardo, E. D., Wang, H., Beddington, R., Skarnes, W. C. and Tessier-Lavigne, M.** (1996). Netrin-1 is required for commissural axon guidance in the developing vertebrate nervous system. *Cell* **87**, 1001-1014.

**Sher, A. E.** (1971). The embryonic and postnatal development of the inner ear of the mouse. *Acta Oto-Laryngol. (Suppl.)* **285**, 1-77.

**Takahashi, K., Kamiya, K., Urase, K., Suga, M., Takizawa, T., Mori, H., Yoshikawa, Y., Ichimura, K., Kuida, K. and Momoi, T.** (2001). Caspase-3-deficiency induces hyperplasia of supporting cells and degeneration of sensory cells resulting in the hearing loss. *Brain Res.* **894**, 359-367.

**Veis, D. J., Sorenson, C. M., Shutter, J. R. and Korsmeyer, S. J.** (1993). Bcl-2-deficient mice demonstrate fulminant lymphoid apoptosis, polycystic kidneys, and hypopigmented hair. *Cell* **75**, 229-249.

**Yang, J., Liu, X., Bhalla, K., Kim, C. N., Ibrado, A. M., Cai, J., Peng, T-I., Jones, D. P. and Wang, X.** (1997). Prevention of apoptosis by Bcl-2: release of cytochrome c from mitochondria blocked. *Science* **275**, 1129-1132.

**Yoshida, H., Kong, Y. Y., Yoshida, R., Elia, A. J., Hakem, A., Hakem, R., Penninger, J. M. and Mak, T. W.** (1998). Apaf1 is required for mitochondrial pathways of apoptosis and brain development. *Cell* **94**, 739-750.

**Yoshida, H., Okada, Y., Kinoshita, N., Hara, H., Sasaki, M., Sawa, H., Nagashima, K., Mak, T. W., Ikeda, K. and Motoyama, N.** (2002). Differential requirement for Apaf1 and Bcl-XL in the regulation of programmed cell death during development. *Cell Death Differ.* **9**, 1273-1276.

**Yuan, J. and Yankner, B. A.** (2000). Apoptosis in the nervous system. *Nature* **407**, 802-809.